Main Manuscript for

The mouse gut microbiota responds to predator odor and predicts host behavior

Madalena V. F. Real[1,2,*], Maren N. Vitousek[1], Michael J. Sheehan[3], Andrew H. Moeller[1,2,*].

[1] Department of Ecology and Evolutionary Biology, Cornell University, Ithaca, NY 14853, USA.

[2] Department of Ecology and Evolutionary Biology, Princeton University, Princeton, NJ 08544, USA.

[3] Department of Neurobiology and Behavior, Cornell University, Ithaca, NY 14853, USA.

[*]Madalena V. F. Real and Andrew H. Moeller.

Email: mv469@cornell.edu or andrew.moeller@princeton.edu

Abstract

Chronic stressors can alter the mammalian gut microbiota in ways that mediate host stress responses, but the impacts of acute stressors on these interactions are less well understood. Here, we show that brief exposure of wild-derived mice to predator odor altered gut-microbiota composition, which in turn predicted host behavior. We investigated the individual and combined effects of 15-minute exposures to synthetic fox fecal odor and 30 days of chronic social isolation, an established chronic stressor. Using ethological assays, visceral adipose tissue transcriptomics, and genome-resolved metagenomics, we found that predator-odor exposure significantly affected mouse behavior, gene expression, and gut microbiota. Predator odor–responsive bacteria were associated with the expression of genes involved in anti-microbial defense, and host behavioral responses were predicted by random forest models trained on gut-microbiota profiles. These findings indicate interactions between the gut microbiota and wild-mouse responses to the threat of predation, an ecologically relevant acute stressor.

Introduction

Animals are faced with diverse stressors that vary in duration and intensity[1,2], giving rise to distinct physiological and behavioral responses[3,4]. In mammals, behavioral[5-7], endocrine[8,9], and immune[5,10,11] stress responses are mediated in part by the community of host-associated microorganisms that reside in the gastrointestinal tract, i.e., the gut microbiota[12], which is shaped by changes in the internal and external host environment[13-15]. Recent work has shown that chronic stressors, such as social isolation, can alter the gut microbiota in ways that mediate host stress responses[16-20]. In contrast, the effects of acute stressors on the gut microbiota, and the relationships between the gut microbiota and host responses to acute stress, remain less well-understood.

In rodents, the threat of predation represents an intense acute stressor, and animals have evolved to use environmental cues, such as predator-odor marks, to adjust their behavior and avoid predator encounters[21]. Previous work in mice has shown that a single brief exposure to synthetic fox fecal odor 2,5-dihydro-2,4,5-trimethylthiazoline (TMT) can

44 lead to long-lasting behavioral changes, such as increased fearfulness[22-26]. However, the
45 effects of acute exposure to predator odor on the gut microbiota, and the extent to which
46 predator odor–induced changes in the gut microbiota interact with host stress responses,
47 have yet to be investigated.

48 Here, we tested the effects of acute exposure to predator odor on the gut microbiota,
49 gene expression, and behavior of wild-derived house mice (*Mus musculus domesticus*) and
50 contrasted these effects with those of social isolation, a well-established chronic stress
51 paradigm. We longitudinally sampled the gut microbiota of males and females exposed to
52 predator odor for 15 minutes at the beginning of the third and fourth weeks of the
53 experiment or socially isolated for 4 weeks. These wild-derived mice retain a more diverse
54 gut microbiota than do lab mice and have recently been proposed as a solution to the
55 microbiota-related issues around the poor reproducibility and low translational value of
56 laboratory mouse studies[27,28]. We found that brief exposure to predator odor had a greater
57 impact on the gut microbiota than did prolonged social isolation. Additionally, the
58 taxonomic composition of the gut microbiota, but not host gene expression profiles,
59 significantly predicted inter-individual variation in host behavior. These findings support
60 links between the gut microbiota and host responses to acute stressors.

61 **Results**

62 *Predator-odor exposure and social isolation gave rise to stress-associated behaviors*

63 We compared the effects of brief exposure to predator odor to those of prolonged exposure
64 to social isolation—a well-established chronic stress model. All experiments were
65 conducted using wild-derived mice originally captured in Saratoga Springs (New York,
66 USA) in 2012 and subsequently inbred in the lab[29-31]. At the beginning of the experiment
67 (D0), we separated groups of 6-week-old same-sex littermates into pair- and single-housed
68 mice (Figure 1A). Two weeks later (D15), we exposed these mice to 35 μL of either
69 synthetic fox fecal odor (2,5-dihydro-2,4,5-trimethylthiazoline, TMT) or a control scent
70 (deionized water, H_2O) for 15 minutes. We repeated this exposure procedure the following
71 week (D22). The full factorial design produced 9 unstressed control cages (10 male and 8

72 female pair-housed H_2O-exposed mice), 6 predator-odor cages (6 male and 6 female pair-
73 housed TMT-exposed mice), 8 social-isolation cages (3 male and 5 female single-housed
74 H_2O-exposed mice), and 9 cages that experienced both stressors (4 male and 5 female
75 single-housed TMT-exposed mice; Supplementary Data 1).

76 We assessed whether brief predator-odor exposure and prolonged social isolation
77 acted as stressors in wild-derived mice by examining the effects of these treatments on host
78 behavior with linear mixed-effects models (LMM) that accounted for sex, litter, and cage
79 effects (Figure 1B; Table S1). We found that individual exposure to the stressors increased
80 mouse fearfulness, as both pair-housed mice exposed to TMT ($\beta = -0.093 \pm 0.038$, $t(26.6)$
81 $= -2.426$, $p = 0.022$) and socially isolated mice exposed to H_2O ($\beta = -0.084 \pm 0.041$, $t(39.3)$
82 $= -2.039$, $p = 0.048$) significantly reduced occupancy of the exposed central area during
83 the open field test [32] when compared to unstressed controls. Mice that experienced both
84 stressors displayed a non-significant trend toward increased fearfulness ($\beta = -0.072 \pm$
85 0.039, $t(39.9) = -1.831$, $p = 0.075$). We conducted additional pairwise comparisons
86 between the stressor groups but found no significant differences in center occupancy (Table
87 S2). There were also no significant differences in overall locomotion between the treatment
88 groups (Table S1 and S2), indicating that the observed reduction in center occupancy was
89 not due to a decrease in overall movement. These results confirm that, in line with previous
90 work in lab mouse strains[3,16,33], predator-odor exposure and social isolation functioned as
91 stressors that increased fear-associated behaviors in wild-derived mice.

92 Predator-odor exposure has also been shown to lead to a reduction in self-
93 grooming[25], which is part of a suite of behaviors that are inhibited when rodents enter a
94 more vigilant state after the threat of predation[34]. We assessed grooming behavior with the
95 splash test[35], where individual mice were sprayed with a palatable sucrose solution and
96 their grooming behavior measured over the subsequent 5 minutes. Social isolation, but not
97 predator-odor exposure, significantly decreased grooming behavior, such that both socially
98 isolated H_2O-exposed mice ($\beta = -44.327 \pm 20.299$, $t(42.0) = -2.184$, $p = 0.035$) and mice
99 that experienced the combined stressors ($\beta = -39.629 \pm 19.204$, $t(41.9) = -2.064$, $p = 0.045$)
100 spent significantly less time grooming than did unstressed controls (Figure 1B; Table S1).

101 There were no significant differences in grooming behavior between stressor treatments
102 (Table S2).
103 Both brief predator-odor exposure[36] and prolonged social isolation[16,33] have been
104 previously reported to decrease rodent sociability, here measured by the relative time spent
105 interacting with a social stimulus (stranger) *versus* a non-social stimulus (empty cup) in
106 the three-chamber test[37]. To assess the sociability of each treatment group, we compared
107 the time each mouse spent interacting with either the social or non-social stimulus using a
108 paired Wilcoxon test. We complemented these analyses with a one-sample Wilcoxon
109 signed-rank test to assess whether the average social preference in each treatment group
110 was significantly different than zero. Finally, we investigated whether the social preference
111 index of mice that experienced the stressors was significantly different than that of controls
112 with a LMM. Contrary to prior work in lab mice[36], we found that pair-housed wild-derived
113 mice exposed to predator odor displayed increased sociability, spending significantly more
114 time interacting with the social stimulus than the non-social stimulus (paired Wilcoxon: V
115 $= 75$, $p = 0.002$; Figure S1) and displaying a social preference index significantly greater
116 than zero (one-sample Wilcoxon: $V = 74$, $p = 0.003$; Figure 1B). In contrast, the social
117 preference index of both groups of single-housed mice or unstressed controls did not differ
118 significantly from zero. While we found no significant differences in the social preference
119 index of mice exposed to the stressors compared to controls (Table S1), the social
120 preference of pair-housed mice exposed to TMT was significantly higher than that of their
121 single-housed counterparts ($\beta = 0.513 \pm 0.197$, $t = 2.610$, FDR-adjusted $p = 0.027$). We did
122 not observe significant sex differences in any of the assayed behaviors (Table S1). Overall,
123 our results show that both brief exposure to predator odor and prolonged social isolation
124 resulted in an increase in stress-related behaviors of wild-derived mice (i.e., fearfulness
125 and, in the case of socially isolated mice, reduced self-grooming), and that predator-odor
126 exposure in the context of pair housing increased sociability.
127

128 *Predator-odor exposure altered the transcriptome of an immunological tissue*

129 Given the observed effects of brief exposure to predator odor and prolonged social isolation
130 on the behaviors of wild-derived mice, we next investigated the impacts of these stressors

131 on gene expression profiles in the visceral adipose tissue (VAT). Both acute and chronic
132 stressors have been shown to increase gut permeability, leading to the translocation of
133 microbes and their metabolites from the gut lumen to surrounding tissues[38], such as the
134 VAT. As an immunologically active organ[39], the VAT can detect these microbial signals[40]
135 and inhibit bacterial infection and sepsis[41,42] through the secretion of anti-microbial
136 peptides (AMPs)[43,44]. To investigate possible effects of the stressors on gene expression
137 profiles, we used 3' RNA-seq to sequence the transcriptomes of VAT collected at the end
138 of the experiment (D33). A total of 35 samples met our quality threshold of over 1 million
139 transcripts/sample, averaging 6.54 million (SD = 3.22 million) transcripts/sample
140 (Supplementary Data 2).

141 We found that TMT exposure, but not social isolation, significantly altered the VAT
142 gene expression profile (PERMANOVA of Euclidean distances accounting for sex and
143 litter; predator odor: $R^2 = 0.047$, $F(1) = 2.185$, $p = 0.035$; social isolation: $R^2 = 0.037$, $F(1)$
144 $= 1.681$, $p = 0.097$; Figure S2; Table S3). We tested for differentially expressed genes
145 (DEGs; absolute $\log_2$(fold change) (LFC) > 1 and FDR-adjusted $p < 0.01$; Supplementary
146 Data 3) between mice exposed to individual stressors and unstressed controls. While there
147 was considerable overlap in DEGs between the different stressor treatments (Figure S3),
148 we found that, compared to social isolation, predator-odor exposure led to a greater number
149 of DEGs (Figures 1C and S3) and a significantly larger mean fold-change in gene
150 expression (unpaired Wilcoxon test $p = 0.026$; Figure S4). Interestingly, DEGs up-
151 regulated in both TMT-exposed (FDR-adjusted $p = 0.007$) and socially isolated mice
152 (FDR-adjusted $p = 0.004$) were significantly enriched in biological pathways related to
153 anti-microbial humoral immune responses, including those mediated by anti-microbial
154 peptides (AMPs; Figure 1D; Table S4). These results show that while both stressors
155 activated anti-microbial defenses, brief predator-odor exposure had a greater overall impact
156 on VAT gene expression than did prolonged social isolation.
157

158 *Predator-odor exposure had a greater impact on the gut microbiota than did social*
159 *isolation*

160 We assessed the impacts of brief exposure to predator odor and prolonged social isolation
161 on the gut microbiota by sequencing the metagenomes of fecal samples collected at the
162 beginning (D0) of the experiment, immediately before the TMT exposures (D15 and D22),
163 and the end of the experiment (D30; Figure 1A; Supplementary Data 4A). Sequencing D0
164 and D30 samples yielded a mean of 33.6 million (SD = 5.0 million) reads/sample.
165 Intermediate samples from D15 and D22 were sequenced at lower depth, yielding a mean
166 of 10.0 million (SD = 2.4 million) reads/sample. We assembled and binned D0 and D30
167 reads into metagenome-assembled genomes (MAGs) using a custom automated workflow
168 (MAGmaker), following previously published methods[45]. The MAGmaker workflow
169 yielded 6,404 MAGs, 3,542 of which were high quality (>90% completeness, <5%
170 contamination). We then created a custom database of 173 representative species-level
171 genome bins (SGBs) by dereplicating high-quality MAGs at 95% average nucleotide
172 identity (ANI). SGBs were classified with the Genome Taxonomy Database[46,47]
173 (Supplementary Data 4B), and their relative abundances in all samples were quantified
174 using InStrain[48] (Supplementary Data 4C). The mean mappability of our samples to the
175 SGBs was 75.75% (SD = 3.04%), indicating that the custom-made SGB database was
176 generally representative of the bacterial diversity in our samples. Samples were rarefied to
177 the minimum library size before beta-diversity analyses (8,470,661 reads for D0 and D30
178 samples, and 3,896,354 reads for D15 and D22 samples; Supplementary Data 4D).

179 We tested the effects of predator-odor exposure and social isolation on the SGB
180 profile through PERMANOVA analyses of Bray-Curtis dissimilarities, accounting for sex,
181 litter, and cage effects. While social isolation significantly affected the mean SGB
182 composition at D22 (PERMANOVA $R^2 = 0.029$, $F(1) = 2.546$, FDR-adjusted $p = 0.008$),
183 this effect disappeared a week later (PERMANOVA $R^2 = 0.011$, $F(1) = 1.282$, FDR-
184 adjusted $p = 0.277$; Figure S5). Instead, at D30, social isolation tended to increase inter-
185 host variance in microbiota composition (PERMDISP $F(1) = 5.754$, FDR-adjusted $p =$
186 0.076). In contrast, TMT exposure impacted the gut microbiota not by changing its inter-
187 individual variance (PERMDISP $F(1) = 0.006$, FDR-adjusted $p = 0.936$) but by

188 significantly shifting the mean SGB composition compared to H_2O exposure
189 (PERMANOVA $R^2 = 0.026$, $F(1) = 2.930$, FDR-adjusted $p = 0.008$). No such effects were
190 observed before predator-odor exposure at D0 and D15 (Table S5).

191 To further examine the effects of stressor exposure while controlling for potential
192 confounding variables, we performed a distance-based redundancy analysis (db-RDA), a
193 constrained ordination approach that tests whether variation in gut-community
194 composition can be explained by predator-odor exposure or social isolation after
195 accounting for sex and litter effects. We found that TMT exposure (PERMANOVA partial
196 $R^2 = 0.057$, $F(1) = 1.992$, $p = 0.024$), but not single housing (PERMANOVA partial $R^2 =$
197 0.027, $F(1) = 0.900$, $p = 0.558$), drove a significant shift in the SGB profile of mice sampled
198 one week after the second TMT exposure (D30; Figure 1E). Overall, these results indicate
199 that two acute exposures to TMT were sufficient to shift the SGB profiles of the mouse gut
200 microbiota, and that by the end of the experiment, the impacts of brief predator-odor
201 exposure on gut-microbiota composition were greater than those of prolonged social
202 isolation.

203

204 *Predator-odor exposure drove consistent alterations in the relative abundances of specific*
205 *SGBs*

206 Given the observed changes in gut-microbiota composition following predator-odor
207 exposure, we investigated which specific microbial taxa drove these patterns. We found
208 that a single exposure to TMT was sufficient to significantly alter the relative abundances
209 of several SGBs (D22 absolute LFC > 1 and FDR-adjusted $p < 0.01$; Figure 2A;
210 Supplementary Data 5). Seven of these SGBs remained differentially abundant (DA) one
211 week after the second TMT exposure (D30), with the majority being enriched in TMT-
212 exposed mice and only one in H_2O-exposed mice (Figures 2A and 2B). In contrast, seven
213 out of the eight SGBs that responded consistently to social isolation were enriched in pair-
214 housed mice, with only one SGB enriched in single-housed individuals (Figures 2A and
215 2B). The latter, SGB158, was the only species consistently enriched in both stressor groups,
216 suggesting a shared response, while most other consistently responsive SGBs showed
217 stressor-specific patterns of enrichment. These findings indicate that a subset of SGBs in

218 the gut microbiota of wild-derived mice displayed consistent changes in abundance in
219 response to brief predator-odor exposure and prolonged social isolation across two
220 timepoints (D22 and D30).

221

222 *Stressor–responsive SGBs co-varied with host anti-microbial and behavioral responses*

223 As the stressors up-regulated the expression of genes involved in AMP production, we
224 investigated possible associations between the expression of these AMP-associated genes
225 and the relative abundances of bacteria that responded consistently to predator-odor
226 exposure or social isolation. We conducted these analyses both across and within treatment
227 groups. In the within-group analyses, we controlled for the effects of the stressor treatments
228 by testing associations with partial Spearman correlations, that residualized host
229 phenotypes (i.e., AMPs expression levels and behavior) and SGB relative abundances
230 against each treatment group. We found that, a week after the first predator-odor exposure
231 (D22), TMT-responsive SGBs generally showed positive associations with genes involved
232 in AMP production, although, after correcting for multiple testing, this correlation was only
233 significant for SGB074—identified as Oscillospiraceae species *Pelethomonas* sp.
234 009774055 (Figure 3). Interestingly, TMT-responsive SGB105—identified as
235 Lachnospiraceae species *Acetatifactor* sp. 011959105—was negatively associated with all
236 genes involved in AMP production. This inverse relation with anti-microbial immune
237 responses was also found in SGBs depleted in mice exposed to the stressors, such
238 SGB051—identified as Muribaculaceae species *Lepagella* sp. 002361155 and enriched in
239 H_2O-exposed mice—as well as most SGBs that consistently responded to pair-housing
240 (Figure S6). These results show that the relative abundances of stressor–responsive SGBs
241 were significantly associated with host anti-microbial defenses.

242 We also tested whether the relative abundances of stressor–responsive SGBs co-
243 varied with host behavioral responses. We found that within-group variation in D22
244 relative abundances of all stressor–responsive SGBs except SGB158 were negatively
245 associated with mouse social preference (Figures 3 and S6). Instead, this Lachnospiraceae
246 species, enriched in both TMT-exposed and socially isolated mice, was negatively
247 correlated with grooming behavior. These findings indicate that behavioral responses to

248 stressor exposure, such as reduced grooming and social preference (particularly for single-
249 housed mice exposed to TMT), could be partially explained by the relative abundances of
250 stressor-responsive SGBs measured a week prior.

251

252 *Gut microbiota predicted host behavioral responses to stressors*

253 Motivated by the observation that host phenotypes could be partially explained by the
254 relative abundances of specific stressor-responsive SGBs, we tested the predictive power
255 of the entire gut microbiota. Variation in gut microbial communities has been shown to
256 shape host behavioral responses to stress[5-7]. Here, we aimed not to infer causality directly
257 but to assess whether inter-individual differences in gut microbiota composition contain
258 information that can be used to predict variation in host behavior both across and within
259 treatment groups. To this end, we trained random forest models to predict host behavior
260 based on SGB relative abundances at each timepoint. For within-group analyses, the
261 predicted behavioral variables were residualized against stressor treatment. The model's
262 performance was assessed through a 5-fold cross-validation strategy, and we conducted a
263 permutation test to measure the statistical significance of the observed R^2 values, which
264 was corrected to account for multiple comparisons across predicted variables and the four
265 timepoints (Table S6). Additionally, we used linear regressions to test the relation between
266 the observed behavioral values and the ones predicted by our models. We found that by the
267 end of our experiment (D30), the gut microbiota consistently predicted grooming and social
268 behavior both across and within treatment groups (Figure 4A). Grooming and fearfulness
269 could also be predicted by inter-individual variation in SGB relative abundances sampled
270 a week prior (D22; Figure S7A). In contrast, the gut microbiota sampled before TMT
271 exposure, at either D0 or D15, was not predictive of host behavior. Interestingly, all SGBs
272 found to respond consistently to predator-odor exposure ranked among the top quarter most
273 important features for predicting at least one of the behavioral phenotypes (Figure 4B;
274 Table S7). For example, the D22 abundance of the predator–odor and social–isolation-
275 responsive SGB158 was the 3rd most important feature for predicting grooming behavior
276 across treatments more than a week later (Figure S7B), corroborating our Spearman
277 correlation results. Furthermore, we found that the gut microbiota was a better predictor of

host behavior than was VAT gene expression, which did not significantly predict behavioral phenotypes (Figure S8; Table S6). These results indicate that the gut microbiota sampled at the end of the experiment, a week after the second TMT exposure, significantly predicted subsequent host behavioral phenotypes.

Discussion

We found that acute exposure of wild-derived mice to predator odor promoted stress-associated behaviors, altered gene expression patterns in the visceral adipose tissue through the activation of the AMP-mediated anti-microbial responses, and shifted the species composition of the gut microbiota. Surprisingly, we found that brief exposure to predator odor had a larger impact on the VAT transcriptome and the gut SGB profile than did prolonged social isolation—a well-established chronic stress model previously shown to impact the gut microbiota[16,17]. Moreover, variation in gut-microbiota composition at the end of the experiment (D30) predicted host behaviors. These results show that predator odor alters the murine gut microbiota and suggest links between inter-individual variation in the gut microbiota and behavioral responses in the context of predation stress.

By comparing the effects of two distinct stressors and their combination on the gut microbiota, host gene expression, and behavior, our study builds on prior work focused on the effects of individual stressors[16,17,49,50]. We observed that the combination of stressors often had non-additive effects, exemplifying the context dependence of the stress response[3]. For example, we observed that pair-housed mice exposed to predator odor displayed significantly higher social preference than did their socially isolated counterparts, demonstrating that the social environment can affect the response to consequent stressors. In our case, pair-housed mice might seek out proximity with conspecifics when under the threat of predation—a behavior described as huddling[51]—while single-housed mice exposed to predator odor display the asocial behavior commonly observed after chronic stressor exposure[52].

Including four treatment groups to test the effects of two stressors and their combination constrained sample sizes. This limitation may have reduced our power to detect, for example, a significant decrease in center occupancy for mice that experienced

307 both stressors compared to controls, or a significant effect of social isolation on gut
308 microbiota composition, as has been previously reported[16,17]. Nevertheless, our group sizes
309 offered sufficient statistical power to detect multiple significant effects of the stressors on
310 mouse behavior, VAT gene expression, and gut microbiota. The biological significance of
311 these results is further supported by the inclusion of both male and female mice in our
312 experimental design, thereby addressing potential sex biases in the stress response[53-55].

313 We identified both general and stressor-specific responses in wild-derived mice and
314 their gut microbiota. For example, we observed that both stressors up-regulated AMP
315 expression in the VAT. Interestingly, the expression of these AMPs co-varied with the
316 relative abundances of stressor-responsive taxa, even after accounting for stressor effects
317 (Figure 3). For example, SGB051, which was depleted in TMT-exposed mice, was
318 negatively associated with all genes involved in AMP production. This SGB was identified
319 as a Muribaculaceae, a family previously associated with anti-inflammatory markers[56,57]
320 and often depleted in inflammatory bowel disease (IBD)[56,58]. Muribaculaceae produce
321 short-chain fatty acids (SCFAs), which have been shown to stimulate mucus production
322 and reduce inflammation[59]. The associations observed in our study could be due to either
323 SGB051 growing better in the absence of AMPs or to a negative effect of this species on
324 anti-microbial responses. One possible explanation for our results is that gut-microbiota
325 responses to predator odor were mediated by VAT inflammation triggered during the acute
326 stress response. Alternatively, it is also possible that predator-odor exposure led to changes
327 in the gut microbiota that triggered VAT inflammation. Given that both increased VAT
328 inflammation[60] and stress-induced changes in the gut microbiota[16,17,61] have been shown to
329 affect mouse behavior, the observed behavioral effects of stressor exposure may be
330 mediated by signaling along the gut-brain-immune axis[62-64]. Alternatively, the gut
331 microbiota may interact with host behavior in a VAT-independent manner, as variation in
332 gut species composition was a better predictor of mouse fearfulness, grooming, and
333 sociability than was the VAT gene expression profile. Understanding the mechanisms
334 underlying the associations between the predation stress–altered microbiota, host
335 inflammatory responses, and behavior will require controlled experiments in germ-free
336 animals designed to test the effects of stressor-associated microbiota on mouse phenotypes

337 that can complement previous work showing that host responses to acute stressors are
338 microbiota-dependent[65-67].

339 Several results contradicted expectations based on previous literature using lab
340 mouse strains. For example, while four weeks of social isolation was sufficient to alter the
341 gut microbiota of C57BL6 males[16,17], in our study, only predator-odor exposure
342 significantly shifted the mean species composition of the gut microbiota at D30. This
343 discrepancy could be due to differences in the robustness of the gut community to
344 perturbation between mouse strains. Lab mice have a depleted, and potentially more
345 volatile, gut microbiota compared to wild mice[27,28], and previous work has shown that wild-
346 derived mouse lines can retain microbiota from wild populations for over a dozen
347 generations in the lab[68]. Additionally, there is evidence that wild-derived mice are less
348 sociable than lab mouse strains[69-71], potentially increasing their tolerance for social
349 isolation. This hypothesis is supported by our observation that unstressed controls lack a
350 clear social preference, whereas commonly used lab lines tend to display high sociability[72].
351 The sociability displayed by pair-housed wild-derived mice exposed to predator odor
352 similarly contradicts findings of previous studies of lab mice[36]. Brief predator-odor
353 exposure is likely a more potent stressor for wild-derived mice than prolonged social
354 isolation. This is supported by previous work showing wild-derived mice are more readily
355 responsive to the threat of predation than lab mice[73]. Thus, this work adds to a growing
356 body of evidence motivating the incorporation of wild-derived mice into research as a
357 biologically relevant complement to the work conducted on classic lab strains[27,28,69,74].
358 Moreover, our results show that acute stressors, such as predator-odor exposure, can have
359 effects of comparable or even greater magnitude than a well-established chronic stressor
360 like social isolation.

361

362 **Materials and Methods**

363 All procedures conformed to guidelines established by the U.S. National Institutes of
364 Health and have been approved by the Cornell University Institutional Animal Care and
365 Use Committee (protocol #2015-0060).

366 Animals

367 We used a wild-derived *M. m. domesticus* line, NY3, which was captured in Saratoga
368 Springs (NY, USA) in 2012 and subsequently inbred in captivity[29-31]. These mice are
369 related to the SAR/NachJ lines currently provided by the Jackson Laboratory[74]. Mice were
370 kept on an inverted light cycle (light:10pm-10am) and all handling was conducted during
371 the active (dark) phase using red light. Standard chow diet and water were available *ad*
372 *libitum*.

373 Stressor Treatments

374 *Social Isolation*

375 Mice were weaned at 3 weeks of age (M = 22 days old, SD = 2) and co-housed with same-
376 sex littermates. At 6 weeks of age (D0; M = 37 days old, SD = 8), we separated co-housed
377 same-sex littermates into pair- and single-housed mice, in a total of 8 male and 7 female
378 mouse pairs, and 7 male and 10 female mice that were socially isolated.

379 *Predator-Odor Exposure*

380 Two weeks after the start of the experiment (D15; M = 57 days old, SD = 5), we exposed
381 mice to synthetic fox fecal odor, 2,5-dihydro-2,4,5-trimethylthiazoline (TMT) (90% purity;
382 BioSRQ, Sarasota, FL, USA). Mice were individually placed in an empty cage, brought to
383 a fume hood, and a filter paper with 35 µL of either TMT or deionized water (H_2O) was
384 placed on their cage metal grid topper for 15 minutes. After the exposure period, we
385 removed the filter paper, keeping the mice in the fume hood for an additional 15 minutes
386 to ensure the TMT was removed from the work area. Afterwards, all mice were returned
387 to their home cages. We exposed control mice first and the TMT-treated mice last, to ensure
388 controls never encountered the predator odor. We repeated this exposure procedure the
389 following week (D22; M = 64 days old, SD = 5). In total, 10 males and 11 females were
390 exposed to TMT, while 13 males and 13 females were exposed to H_2O. Considering both
391 stressors, there were 9 pair-housed H_2O-exposed cages (5 male pairs and 4 female pairs),
392 6 pair-housed TMT-exposed cages (3 male pairs and 3 female pairs), 8 single-housed H_2O-
393 exposed cages (3 males and 5 females), and 9 single-housed TMT-exposed cages (4 males
394 and 5 females).

395 Behavioral Assays

396 We assayed mouse behavior on the fifth week of the experiment (D30; M = 72 days old,
397 SD = 6), over three consecutive days. The tests were ordered from least to most disruptive,
398 starting with the Open Field Test (OFT)[32], followed by the Splash Test (SP)[35], and ending
399 with the Three-Chamber Test (3CT). All behavior trials were conducted between 1:00-6:00
400 pm, and as mice were kept on an inverted light cycle, this time corresponded to the animals'
401 active (dark) phase. The OFT and 3CT were conducted inside a soundproof chamber in a
402 separate behavior room. The mice were habituated to the behavior room for at least 30
403 minutes. We alternated the testing order between experimental groups and wiped the
404 behavioral apparatuses between trials with 70% ethanol. An infrared camera placed above
405 the apparatuses recorded the behavior tests. All analyses were conducted by the same
406 experimenter, who was blind to the experimental condition.

407 *Open Field Test*

408 Mice were placed in the center of a white PVC arena (48 × 46 × 44 cm) and allowed to
409 explore for 10 minutes. We used ToxTrac[75] to detect mouse trajectories and calculate total
410 distance walked and time spent in the center of the arena (34 × 32 cm; ½ of the area). After
411 the test, each mouse was housed in a new individual home cage.

412 *Splash Test*

413 Our protocol was adapted from Nollet [76]. On the second day of behavior tests, each mouse
414 was placed in an empty "spray" cage and sprayed on their dorsal coat with a 10% sucrose
415 solution. Mice were then quickly returned to their home cage, and grooming behavior was
416 measured for the following 5 minutes. We directly measured the duration of the grooming
417 behavior by using a chronometer to time observed instances of nose/face grooming, head
418 washing, and body grooming, as described by Kalueff and Tuohimaa [77].

419 *Three-Chamber Test*

420 Mice were placed in the middle chamber of a transparent plexiglass three-chamber arena
421 for a 5-minute habituation period. We then placed overturned wire cups on diagonally
422 opposite corners of each side chamber. One of the cups was empty (non-social stimulus),
423 while the other contained a stranger mouse of the same sex as the test mouse (social

424 stimulus). The position of the stimuli was counterbalanced between trials. We allowed the
425 test mouse to explore the arena for 10 minutes. The recorded video footage was manually
426 scored with BORIS where we logged interactions with the social and non-social stimuli
427 following recommendations by Rein, et al. [37]. These were behaviors such as directly
428 interacting with the stranger mouse between the cup's wire bars and/or sniffing the cup or
429 any protruding part of the stranger mouse (e.g., tail). Climbing on top of the cups or
430 grooming in their proximity was not counted as an interaction. Additionally, we calculated
431 the social preference index, which is the difference in interaction time between the social
432 and non-social stimulus, normalized by the total time interacting with both stimuli [37].
433 Significantly higher interaction time with the social *versus* non-social stimulus was
434 interpreted as the existence of a social preference[37].

435 Host Gene Expression

436 *Tissue Collection and Gross Morphometry*

437 Mice were humanely euthanized with an overdose of CO_2 followed by cervical dislocation.
438 Immediately after, we dissected the visceral adipose tissue (VAT), which was flash frozen
439 and stored at -80°C.

440 *Transcriptomic Sequencing*

441 Total RNA was extracted from the VAT using the RNeasy Lipid Tissue Mini Kit (Qiagen,
442 Germantown, MD, USA). Briefly, approximately 50 mg of VAT were placed in Bead
443 Ruptor 2 mL tubes with 2.4 mm metal beads (Omni International, Kennesaw, GA, USA)
444 and 1 mL of QIAzol Lysis Reagent (Qiagen). The tissues were homogenized with a Bead
445 Ruptor (Omni International) at speed 5 for 30 seconds. We followed the manufacturer's
446 instructions for the remainder of both RNeasy protocols, including the optional drying step
447 of placing the RNeasy spin column in a new 2 mL collection tube and centrifuging at full
448 speed for 1 minute. Total RNA was eluted twice in 30 µL of RNase-free water (Qiagen).
449 We assessed the concentration and purity of the extracted RNA with a NanoDrop
450 Microvolume Spectrophotometer (Thermo Fisher Scientific) for all samples and with a
451 TapeStation (Agilent Technologies, Santa Clara, CA, USA) for 10% of the samples. The

452 3'RNA-seq libraries were prepared at Cornell University's Biotechnology Resource Center
453 (BRC; Ithaca, NY, USA) and sequenced on a NextSeq 500 (Illumina).

454 *Transcriptomic Data Processing*

455 We assessed the quality of our transcriptomic data with FastQC (v0.72.0)[78] and filtered out
456 samples with fewer than 1 million reads. The remaining transcripts were aligned against
457 the *Mus musculus* reference genome (GRCm39 GCF_000001635.27) using STAR
458 (v2.7.10b; setting: --quantMode GeneCounts --outSAMtype BAM SortedByCoordinate)[79].

459 Gut Microbiota

460 *Fecal Collections*

461 We sequenced the metagenome from fecal samples collected at the beginning of the first
462 (D0), third (D15), fourth (D22), and fifth (D30) weeks of the experiment. D15 and D22
463 samples were collected immediately before the predator-odor exposure procedure. D30
464 samples were collected immediately before the first behavioral assay. All fecal samples
465 were flash frozen and stored at -80°C.

466 *DNA Sequencing*

467 Total microbial DNA was extracted with the Quick-DNA MagBead extraction kit (Zymo,
468 Irvine, CA, USA) using an OT-2 liquid handling robot (Opentrons, New York, NY, USA).
469 The metagenomic libraries were prepared with the TruSeq kit (Illumina, San Diego, CA,
470 USA) at Cornell's BRC. The D0 and D30 libraries were sequenced in a NovaSeq 6000 S4
471 (PE150 bp; Illumina) at the UC Davis Genome Center (Davis, CA, USA), while the D15
472 and D22 libraries were sequenced in a NovaSeq X (2 × 150 bp; Illumina) at Cornell's BRC.

473 *Metagenomic Data Processing and Analysis*

474 We processed our metagenomic samples and assembled MAGs using a custom
475 snakemake[80] workflow (MAGmaker)[45]. Briefly, sequencing adapters were trimmed with
476 Cutadapt (v17.4; setting: "-a AGATCGGAAGAGCACACGTCTGAACTCCAGTCA -A
477 AGATCGGAAGAGCGTCGTGTAGGGAAAGAGTGT -a
478 GGGGGGGGGGGGGGGGGGGG -A GGGGGGGGGGGGGGGGGGGG -u 10 -U 10 -

479 -minimum-length 1 --nextseq-trim 20")[81], host reads removed with Bowtie2 (v2.5.1;
480 setting: "--very-fast"; host reference genome: GRCm39 GCF_000001635.27)[82], and the
481 quality of our metagenomic data was assessed with FastQC (v0.72.0)[78]. We assembled
482 high-quality non-host reads from D0 and D30 into contiguous sequences (contigs) using
483 Megahit (v1.2.9)[83] and assessed assembly quality with Quast (v5.2.0)[84]. We then calculated
484 the distances between our samples using SourMash (v4.4.0)[85] and selected the 11 samples
485 most dissimilar to all others to be used as "prototypes" against which the metagenomic
486 reads from all samples were mapped with Minimap2 (v2.24)[86]. The resulting coverage
487 information was input into three different binning algorithms: CONCOCT (v0.4.2)[87],
488 MetaBAT2 (v2.15)[88], and MaxBin (v2.2)[89]. We then used DASTool (v1.1.6)[90] to select the
489 optimal set of bins among the three binners. The resulting MAGs were quality controlled
490 for completeness and contamination with CheckM (v1.2.2)[91] and GUNC (v1.0.6)[92]. We
491 created a custom genome database by dereplicating high-quality MAGs (>90%
492 completeness, <5% contamination) into 95% average nucleotide identity (ANI) species-
493 genome bins (SGBs) using dRep (v3.4.2)[93]. We profiled these SGBs using GTDB-Tk
494 (v2.4.0)[47]. Finally, we calculated the relative abundances of representative SGBs in our
495 samples by mapping all metagenomic reads against our custom genome database with
496 Bowtie2 and profiling them using InStrain (v1.8.0)[48]. The counts from our mapped reads
497 were normalized by the genome size of the representative SGB the read mapped to and the
498 library size of the metagenomic sample from which the read originated. We then converted
499 these normalized counts into a relative abundance percentage. The Bray-Curtis
500 dissimilarities between samples were calculated using methods from the 'vegan' package
501 (v2.6)[94] via 'phyloseq' (v1.42.0)[95].

502 Statistical Analyses

503 All data analyses, except were indicated, were conducted in R (v4.2.2). Means (M) are
504 reported alongside standard deviations (SD). Linear mixed-effects models, controlling for
505 litter and cage as a random effect (formula: Behavior ~ Sex + Treatment +
506 (1|Litter/Cage_ID)), were implemented via 'lmerTest' (v3.1)[96]. Statistical results are
507 shown as estimate (β) ± standard error (SE), followed by *t*-value (with corresponding
508 degrees of freedom), and *p*-value. Pairwise comparisons between stressor treatments were

509 calculated using the 'multcomp' package (v1.4-25)[97]. We tested which factors explained
510 the microbiota dissimilarity matrix by running a PERMANOVA [98] via adonis2 (formula:
511 Dissimilarity matrix ~ Sex + Litter + Housing + TMT + Cage) and a PERMDISP[99] via
512 betadisper, both included in 'vegan' (v2.6)[94]. Statistical results are shown in-text as *F*
513 statistic (with corresponding degrees of freedom), R^2 (applicable to the PERMANOVA,
514 but not PERMDISP), and FDR-adjusted *p*-value to account for the hypothesis testing being
515 repeated across four different timepoints. We calculated normalized counts and differential
516 gene expression or taxa relative abundances between stressor treatments using 'DESeq2'
517 (v1.42.1; formula: ~ Sex + Housing * TMT + Litter)[100] with LFC shrinkage using the
518 "ashr" adaptive shrinkage estimator[101], after filtering for genes or taxa with one or more
519 counts in at least three samples. We identified biologically meaningful pathways within
520 DEGs with an enrichment analysis using 'clusterProfiler' (v4.10.1)[102]. We investigated
521 whether species relative abundances significantly explained variation in behavior while
522 controlling for stressor treatment effects with a random forest model implemented via
523 Python's 'scikit-learn' (v1.6)[103]. We evaluated our model's performance using a 5-fold
524 cross-validation strategy, where we subset our data into 5 different "folds" and trained the
525 model 5 times, using 4 of the folds as the training data and the remaining fold as the test
526 data. Our performance metric (R^2) was averaged across all 5 iterations. This way, each data
527 point is used at least once to both train and test our model, and the R^2 reflects the model's
528 performance across the entire dataset. We evaluated the statistical significance of the R^2
529 using a permutation test, where we randomized the associations between behavior and
530 species relative abundances and recalculated R^2 for 1000 iterations, thus generating a
531 distribution of R^2 values expected under the null hypothesis that behavior is not associated
532 with species relative abundances. We calculated a *p*-value by measuring the likelihood of
533 observing the R^2 resultant from our random forest in the null distribution. Lastly, we
534 assessed the importance of individual SGBs in predicting behavior using Python's 'scikit-
535 learn' (v1.6)[103]. Throughout the analyses, a $p < 0.05$ was considered statistically significant,
536 except where otherwise indicated. All plots were created with 'ggplot2' (v3.4.1)[104]. All
537 figure panels were assembled using Inkscape 1.2.

538 **Author Contributions**

539 M.V.F.R., Conceptualization, Methodology, Investigation, Formal analysis,
540 Visualization, Writing – original draft, Writing – review & editing; M.N.V.,
541 Conceptualization, Methodology, Writing – review & editing; M.J.S., Conceptualization,
542 Methodology, Investigation, Writing – review & editing; A.H.M., Conceptualization,
543 Methodology, Investigation, Formal analysis, Visualization, Writing – original draft,
544 Writing – review & editing, Funding acquisition.

545 **Acknowledgments**

546 Funding was provided by the National Institutes of Health (NIH) grants R35 GM138284
547 and R01 DK139214 to A.H.M. NIH had no role in study design, data collection, and
548 interpretation, or the decision to submit the work for publication. We acknowledge
549 Cornell's Biotechnology Resource Center for the help with sequencing host
550 transcriptomic and fecal metagenomic data. We also thank Sylvia Bayrakdarian for her
551 help with the animal care and behavioral tests.

552 **Competing Interests**

553 The authors declare no competing interests.

554 **Data availability**

555 All the FASTQ sequence data and associated metadata have been deposited in NCBI's
556 Sequence Read Archive under accession no. PRJNA1271077. Code for all analyses
557 conducted in this manuscript is available at
558 https://github.com/CUMoellerLab/Real_etal_2025_Predator_Stress.

References

1 Romero, L. M., Dickens, M. J. & Cyr, N. E. The Reactive Scope Model - a new model integrating homeostasis, allostasis, and stress. *Horm Behav* **55**, 375-389, doi:10.1016/j.yhbeh.2008.12.009 (2009).

2 Del Giudice, M. *et al.* What Is Stress? A Systems Perspective. *Integr Comp Biol* **58**, 1019-1032, doi:10.1093/icb/icy114 (2018).

3 Du Preez, A. *et al.* The type of stress matters: repeated injection and permanent social isolation stress in male mice have a differential effect on anxiety- and depressive-like behaviours, and associated biological alterations. *Transl Psychiatry* **10**, 325, doi:10.1038/s41398-020-01000-3 (2020).

4 Du Preez, A. *et al.* Do different types of stress differentially alter behavioural and neurobiological outcomes associated with depression in rodent models? A systematic review. *Front Neuroendocrinol* **61**, 100896, doi:10.1016/j.yfrne.2020.100896 (2021).

5 Pearson-Leary, J. *et al.* The gut microbiome regulates the increases in depressive-type behaviors and in inflammatory processes in the ventral hippocampus of stress vulnerable rats. *Mol Psychiatry* **25**, 1068-1079, doi:10.1038/s41380-019-0380-x (2020).

6 Chevalier, G. *et al.* Effect of gut microbiota on depressive-like behaviors in mice is mediated by the endocannabinoid system. *Nat Commun* **11**, 6363, doi:10.1038/s41467-020-19931-2 (2020).

7 Ritz, N. L. *et al.* Social anxiety disorder-associated gut microbiota increases social fear. *Proceedings of the National Academy of Sciences* **121**, e2308706120 (2023).

8 de Weerth, C. Do bacteria shape our development? Crosstalk between intestinal microbiota and HPA axis. *Neurosci Biobehav Rev* **83**, 458-471, doi:10.1016/j.neubiorev.2017.09.016 (2017).

9 Mir, H. D. *et al.* The gut microbiota metabolite indole increases emotional responses and adrenal medulla activity in chronically stressed male mice. *Psychoneuroendocrinology* **119**, 104750, doi:10.1016/j.psyneuen.2020.104750 (2020).

10 Agranyoni, O. *et al.* Gut microbiota determines the social behavior of mice and induces metabolic and inflammatory changes in their adipose tissue. *NPJ Biofilms Microbiomes* **7**, 28, doi:10.1038/s41522-021-00193-9 (2021).

11 Werbner, M. *et al.* Social-Stress-Responsive Microbiota Induces Stimulation of Self-Reactive Effector T Helper Cells. *mSystems* **4**, doi:10.1128/mSystems.00292-18 (2019).

12 Weiss, S. Microbiota as mediator and moderator of stress. *Bioessays* **43**, e2000277, doi:10.1002/bies.202000277 (2021).

13 Moeller, A. H. & Sanders, J. G. Roles of the gut microbiota in the adaptive evolution of mammalian species. *Philos Trans R Soc Lond B Biol Sci* **375**, 20190597, doi:10.1098/rstb.2019.0597 (2020).

14 Candela, M., Biagi, E., Maccaferri, S., Turroni, S. & Brigidi, P. Intestinal microbiota is a plastic factor responding to environmental changes. *Trends in microbiology* **20**, 385-391 (2012).

15 David, L. A. *et al.* Host lifestyle affects human microbiota on daily timescales. *Genome biology* **15**, 1-15 (2014).

601 16 Huang, L. *et al.* Commensal microbe-derived propionic acid mediates juvenile social
602 isolation-induced social deficits and anxiety-like behaviors. *Brain Research Bulletin* **166**,
603 161-171 (2021).
604 17 Usui, N., Matsuzaki, H. & Shimada, S. Characterization of Early Life Stress-Affected
605 Gut Microbiota. *Brain sciences* **11**, 913 (2021).
606 18 Siopi, E. *et al.* Changes in gut microbiota by chronic stress impair the efficacy of
607 fluoxetine. *Cell Reports* **30**, 3682-3690. e3686 (2020).
608 19 Wang, P. *et al.* Gut microbiome-derived ammonia modulates stress vulnerability in the
609 host. *Nat Metab* **5**, 1986-2001, doi:10.1038/s42255-023-00909-5 (2023).
610 20 Ritz, N. L. *et al.* The gut virome is associated with stress-induced changes in behaviour
611 and immune responses in mice. *Nature Microbiology* **9**, 359-376 (2024).
612 21 Apfelbach, R., Blanchard, C. D., Blanchard, R. J., Hayes, R. A. & McGregor, I. S. The
613 effects of predator odors in mammalian prey species: a review of field and laboratory
614 studies. *Neuroscience & Biobehavioral Reviews* **29**, 1123-1144 (2005).
615 22 Baumbach, J. L., Mui, C. Y., Zahra, F. T. & Martin, L. J. A single exposure to the
616 predator odor 2, 4, 5-trimethylthiazoline causes long-lasting affective behavioral changes
617 in female mice: Modulation by kappa opioid receptor signaling. *Pharmacology*
618 *Biochemistry and Behavior* **242**, 173822 (2024).
619 23 Post, R. J., Dahlborg, K. M., O'Loughlin, L. E. & Bloom, C. M. Effects of juvenile
620 exposure to predator odor on adolescent and adult anxiety and pain nociception.
621 *Physiology & behavior* **131**, 57-61 (2014).
622 24 Hebb, A. L. *et al.* Brief exposure to predator odor and resultant anxiety enhances
623 mesocorticolimbic activity and enkephalin expression in CD-1 mice. *European Journal*
624 *of Neuroscience* **20**, 2415-2429 (2004).
625 25 Janitzky, K. *et al.* Behavioral effects and pattern of brain c-fos mRNA induced by 2, 5-
626 dihydro-2, 4, 5-trimethylthiazoline, a component of fox feces odor in GAD67-GFP
627 knock-in C57BL/6 mice. *Behavioural brain research* **202**, 218-224 (2009).
628 26 Hebb, A. L. *et al.* Odor-induced variation in anxiety-like behavior in mice is associated
629 with discrete and differential effects on mesocorticolimbic cholecystokinin mRNA
630 expression. *Neuropsychopharmacology* **27**, 744-755 (2002).
631 27 Oh, J. H. & Rehermann, B. Natural versus laboratory world: incorporating wild-derived
632 microbiota into preclinical rodent models. *The Journal of Immunology* **207**, 1703-1709
633 (2021).
634 28 Bruno, P., Schüler, T. & Rosshart, S. P. Born to be wild: utilizing natural microbiota for
635 reliable biomedical research. *Trends in Immunology* (2024).
636 29 Sheehan, M. J., Campbell, P. & Miller, C. H. Evolutionary patterns of major urinary
637 protein scent signals in house mice and relatives. *Molecular ecology* **28**, 3587-3601
638 (2019).
639 30 Miller, C. H. *et al.* Dynamic changes to signal allocation rules in response to variable
640 social environments in house mice. *Communications Biology* **6**, 297 (2023).
641 31 Miller, C. H., Haxhillari, K., Hillock, M. F., Reichard, T. M. & Sheehan, M. J. Scent
642 mark signal investment predicts fight dynamics in house mice. *Proceedings of the Royal*
643 *Society B* **290**, 20222489 (2023).

32 Gould, T. D., Dao, D. T. & Kovacsics, C. E. The open field test. *Mood and anxiety related phenotypes in mice*, 1-20 (2009).
33 Hacquemand, R., Choffat, N., Jacquot, L. & Brand, G. Comparison between low doses of TMT and cat odor exposure in anxiety-and fear-related behaviors in mice. *Behavioural brain research* **238**, 227-231 (2013).
34 Blanchard, R. J., Blanchard, D. C., Rodgers, J. & Weiss, S. M. The characterization and modelling of antipredator defensive behavior. *Neuroscience & Biobehavioral Reviews* **14**, 463-472 (1990).
35 Nollet, M., Guisquet, A. M. L. & Belzung, C. Models of depression: unpredictable chronic mild stress in mice. *Current protocols in pharmacology* **61**, 5.65. 61-65.65. 17 (2013).
36 Zangrossi Jr, H. & File, S. E. Behavioral consequences in animal tests of anxiety and exploration of exposure to cat odor. *Brain research bulletin* **29**, 381-388 (1992).
37 Rein, B., Ma, K. & Yan, Z. A standardized social preference protocol for measuring social deficits in mouse models of autism. *Nat Protoc* **15**, 3464-3477, doi:10.1038/s41596-020-0382-9 (2020).
38 Kelly, J. R. *et al.* Breaking down the barriers: the gut microbiome, intestinal permeability and stress-related psychiatric disorders. *Frontiers in cellular neuroscience* **9**, 392 (2015).
39 Grant, R. W. & Dixit, V. D. Adipose tissue as an immunological organ. *Obesity* **23**, 512-518 (2015).
40 Bertin, B., Desreumaux, P. & Dubuquoy, L. Obesity, visceral fat and Crohn's disease. *Current Opinion in Clinical Nutrition & Metabolic Care* **13**, 574-580 (2010).
41 Karrasch, T. & Schaeffler, A. Adipokines and the role of visceral adipose tissue in inflammatory bowel disease. *Annals of Gastroenterology: Quarterly Publication of the Hellenic Society of Gastroenterology* **29**, 424 (2016).
42 Batra, A. *et al.* Mesenteric fat—control site for bacterial translocation in colitis? *Mucosal Immunology* **5**, 580-591 (2012).
43 Zhang, L.-j. *et al.* Dermal adipocytes protect against invasive Staphylococcus aureus skin infection. *Science* **347**, 67-71 (2015).
44 Alcorn, J. F. & Kolls, J. K. Killer fat. *Science* **347**, 26-27 (2015).
45 Sanders, J. G. *et al.* Widespread extinctions of co-diversified primate gut bacterial symbionts from humans. *Nat Microbiol* **8**, 1039-1050, doi:10.1038/s41564-023-01388-w (2023).
46 Parks, D. H. *et al.* GTDB: an ongoing census of bacterial and archaeal diversity through a phylogenetically consistent, rank normalized and complete genome-based taxonomy. *Nucleic acids research* **50**, D785-D794 (2022).
47 Chaumeil, P.-A., Mussig, A. J., Hugenholtz, P. & Parks, D. H. (Oxford University Press, 2020).
48 Olm, M. R. *et al.* inStrain profiles population microdiversity from metagenomic data and sensitively detects shared microbial strains. *Nat Biotechnol*, doi:10.1038/s41587-020-00797-0 (2021).
49 Patel, K. V. *et al.* Impact of acute stress on the canine gut microbiota. *Scientific Reports* **14**, 18897 (2024).

50 Rodiño-Janeiro, B. K. *et al.* Acute stress triggers sex-dependent rapid alterations in the human small intestine microbiota composition. *Frontiers in Microbiology* **15**, 1441126 (2025).
51 Bowen, M. T. *et al.* Aggregation in quads but not pairs of rats exposed to cat odor or bright light. *Behavioural processes* **90**, 331-336 (2012).
52 Sandi, C. & Haller, J. Stress and the social brain: behavioural effects and neurobiological mechanisms. *Nature reviews neuroscience* **16**, 290-304 (2015).
53 Borrow, A. P., Bales, N. J., Stover, S. A. & Handa, R. J. Chronic Variable Stress Induces Sex-Specific Alterations in Social Behavior and Neuropeptide Expression in the Mouse. *Endocrinology* **159**, 2803-2814, doi:10.1210/en.2018-00217 (2018).
54 Liu, N. *et al.* Single housing-induced effects on cognitive impairment and depression-like behavior in male and female mice involve neuroplasticity-related signaling. *Eur J Neurosci* **52**, 2694-2704, doi:10.1111/ejn.14565 (2020).
55 Guo, M., Wu, C. F., Liu, W., Yang, J. Y. & Chen, D. Sex difference in psychological behavior changes induced by long-term social isolation in mice. *Progress in Neuro-Psychopharmacology and Biological Psychiatry* **28**, 115-121 (2004).
56 Li, A.-l. *et al.* Effect of 2′-fucosyllactose supplementation on intestinal flora in mice with intestinal inflammatory diseases. *International Dairy Journal* **110**, 104797 (2020).
57 Zhan, F., Song, W., Fan, Y., Wang, F. & Wang, Q. Cucurbitacin E Alleviates Colonic Barrier Function Impairment and Inflammation Response and Improves Microbial Composition on Experimental Colitis Models. *Journal of Inflammation Research*, 2745-2756 (2024).
58 Volk, J. K. *et al.* The Nlrp6 inflammasome is not required for baseline colonic inner mucus layer formation or function. *Journal of Experimental Medicine* **216**, 2602-2618 (2019).
59 van der Hee, B. & Wells, J. M. Microbial regulation of host physiology by short-chain fatty acids. *Trends in microbiology* **29**, 700-712 (2021).
60 Guo, D.-H. *et al.* Visceral adipose NLRP3 impairs cognition in obesity via IL-1R1 on CX3CR1+ cells. *The Journal of clinical investigation* **130**, 1961-1976 (2020).
61 Dunphy-Doherty, F. *et al.* Post-weaning social isolation of rats leads to long-term disruption of the gut microbiota-immune-brain axis. *Brain, behavior, and immunity* **68**, 261-273 (2018).
62 Agirman, G., Yu, K. B. & Hsiao, E. Y. Signaling inflammation across the gut-brain axis. *Science* **374**, 1087-1092 (2021).
63 Fung, T. C. The microbiota-immune axis as a central mediator of gut-brain communication. *Neurobiology of disease* **136**, 104714 (2020).
64 Puricelli, C. *et al.* The gut-brain-immune axis in autism spectrum disorders: a state-of-art report. *Frontiers in Psychiatry* **12**, 755171 (2022).
65 Lyte, J. M. *et al.* Gut-brain axis serotonergic responses to acute stress exposure are microbiome-dependent. *Neurogastroenterol Motil* **32**, e13881, doi:10.1111/nmo.13881 (2020).
66 Rosell-Cardona, C. *et al.* Acute stress enhances synaptic plasticity in male mice via a microbiota-dependent mechanism. *Neuropharmacology* **273**, 110434 (2025).

67 Vagnerová, K. *et al.* Interactions between gut microbiota and acute restraint stress in peripheral structures of the hypothalamic–pituitary–adrenal axis and the intestine of male mice. *Frontiers in immunology* **10**, 2655 (2019).

68 Moeller, A. H., Suzuki, T. A., Phifer-Rixey, M. & Nachman, M. W. Transmission modes of the mammalian gut microbiota. *Science* **362**, 453-457, doi:10.1126/science.aat7164 (2018).

69 Vogt, C. C. *et al.* Female behavior drives the formation of distinct social structures in C57BL/6J versus wild-derived outbred mice in field enclosures. *BMC biology* **22**, 35 (2024).

70 Tuttle, A. H. *et al.* Social propinquity in rodents as measured by tube cooccupancy differs between inbred and outbred genotypes. *Proceedings of the National Academy of Sciences* **114**, 5515-5520 (2017).

71 Smith, J., Hurst, J. L. & Barnard, C. Comparing behaviour in wild and laboratory strains of the house mouse: levels of comparison and functional inference. *Behavioural processes* **32**, 79-86 (1994).

72 Moy, S. *et al.* Sociability and preference for social novelty in five inbred strains: an approach to assess autistic-like behavior in mice. *Genes, Brain and Behavior* **3**, 287-302 (2004).

73 Blanchard, R. J. *et al.* Defensive behaviors in wild and laboratory (Swiss) mice: the mouse defense test battery. *Physiology & behavior* **65**, 201-209 (1998).

74 Dumont, B. L. *et al.* Into the Wild: A novel wild-derived inbred strain resource expands the genomic and phenotypic diversity of laboratory mouse models. *PLoS genetics* **20**, e1011228 (2024).

75 Rodriguez, A. *et al.* ToxTrac: a fast and robust software for tracking organisms. *Methods in Ecology and Evolution* **9**, 460-464 (2018).

76 Nollet, M. Models of Depression: Unpredictable Chronic Mild Stress in Mice. *Curr Protoc* **1**, e208, doi:10.1002/cpz1.208 (2021).

77 Kalueff, A. V. & Tuohimaa, P. Grooming analysis algorithm for neurobehavioural stress research. *Brain Research Protocols* **13**, 151-158 (2004).

78 Andrews, S. (Babraham Bioinformatics, Babraham Institute, Cambridge, United Kingdom, 2010).

79 Dobin, A. *et al.* STAR: ultrafast universal RNA-seq aligner. *Bioinformatics* **29**, 15-21 (2013).

80 Mölder, F. *et al.* Sustainable data analysis with Snakemake. *F1000Research* **10** (2021).

81 Martin, M. Cutadapt removes adapter sequences from high-throughput sequencing reads. *EMBnet. journal* **17**, 10-12 (2011).

82 Langmead, B. & Salzberg, S. L. Fast gapped-read alignment with Bowtie 2. *Nature methods* **9**, 357-359 (2012).

83 Li, D., Liu, C.-M., Luo, R., Sadakane, K. & Lam, T.-W. MEGAHIT: an ultra-fast single-node solution for large and complex metagenomics assembly via succinct de Bruijn graph. *Bioinformatics* **31**, 1674-1676 (2015).

84 Gurevich, A., Saveliev, V., Vyahhi, N. & Tesler, G. QUAST: quality assessment tool for genome assemblies. *Bioinformatics* **29**, 1072-1075 (2013).

85 Brown, C. T. & Irber, L. sourmash: a library for MinHash sketching of DNA. *Journal of open source software* **1**, 27 (2016).
86 Li, H. Minimap2: pairwise alignment for nucleotide sequences. *Bioinformatics* **34**, 3094-3100 (2018).
87 Alneberg, J. *et al.* Binning metagenomic contigs by coverage and composition. *Nat Methods* **11**, 1144-1146, doi:10.1038/nmeth.3103 (2014).
88 Kang, D. D. *et al.* MetaBAT 2: an adaptive binning algorithm for robust and efficient genome reconstruction from metagenome assemblies. *PeerJ* **7**, e7359 (2019).
89 Wu, Y. W., Simmons, B. A. & Singer, S. W. MaxBin 2.0: an automated binning algorithm to recover genomes from multiple metagenomic datasets. *Bioinformatics* **32**, 605-607, doi:10.1093/bioinformatics/btv638 (2016).
90 Sieber, C. M. *et al.* Recovery of genomes from metagenomes via a dereplication, aggregation and scoring strategy. *Nature microbiology* **3**, 836-843 (2018).
91 Parks, D. H., Imelfort, M., Skennerton, C. T., Hugenholtz, P. & Tyson, G. W. CheckM: assessing the quality of microbial genomes recovered from isolates, single cells, and metagenomes. *Genome research* **25**, 1043-1055 (2015).
92 Orakov, A. *et al.* GUNC: detection of chimerism and contamination in prokaryotic genomes. *Genome Biol* **22**, 178, doi:10.1186/s13059-021-02393-0 (2021).
93 Olm, M. R., Brown, C. T., Brooks, B. & Banfield, J. F. dRep: a tool for fast and accurate genomic comparisons that enables improved genome recovery from metagenomes through de-replication. *The ISME journal* **11**, 2864-2868 (2017).
94 Oksanen, J. *et al.* Package 'vegan'. *Community ecology package, version* **2**, 1-295 (2013).
95 McMurdie, P. J. & Holmes, S. phyloseq: an R package for reproducible interactive analysis and graphics of microbiome census data. *PloS one* **8**, e61217 (2013).
96 Kuznetsova, A., Brockhoff, P. & Christensen, R. Package 'lmertest'. Version 3.1-0. *Computer software]. Retrieved from https://cran. r-project. org* (2019).
97 Hothorn, T. Multcomp: simultaneous inference in general parametric models. *R package version* **1**, 4 (2020).
98 Anderson, M. J. Permutational multivariate analysis of variance. *Department of Statistics, University of Auckland, Auckland* **26**, 32-46 (2005).
99 Anderson, M. J., Ellingsen, K. E. & McArdle, B. H. Multivariate dispersion as a measure of beta diversity. *Ecology letters* **9**, 683-693 (2006).
100 Love, M. I., Huber, W. & Anders, S. Moderated estimation of fold change and dispersion for RNA-seq data with DESeq2. *Genome biology* **15**, 1-21 (2014).
101 Stephens, M. False discovery rates: a new deal. *Biostatistics* **18**, 275-294 (2017).
102 Wu, T. *et al.* clusterProfiler 4.0: A universal enrichment tool for interpreting omics data. *The Innovation* **2**, 100141 (2021).
103 Pedregosa, F. *et al.* Scikit-learn: Machine learning in Python. *the Journal of machine Learning research* **12**, 2825-2830 (2011).
104 Wickham, H., Chang, W. & Wickham, M. H. Package 'ggplot2'. *Create elegant data visualisations using the grammar of graphics. Version* **2**, 1-189 (2016).

Figures

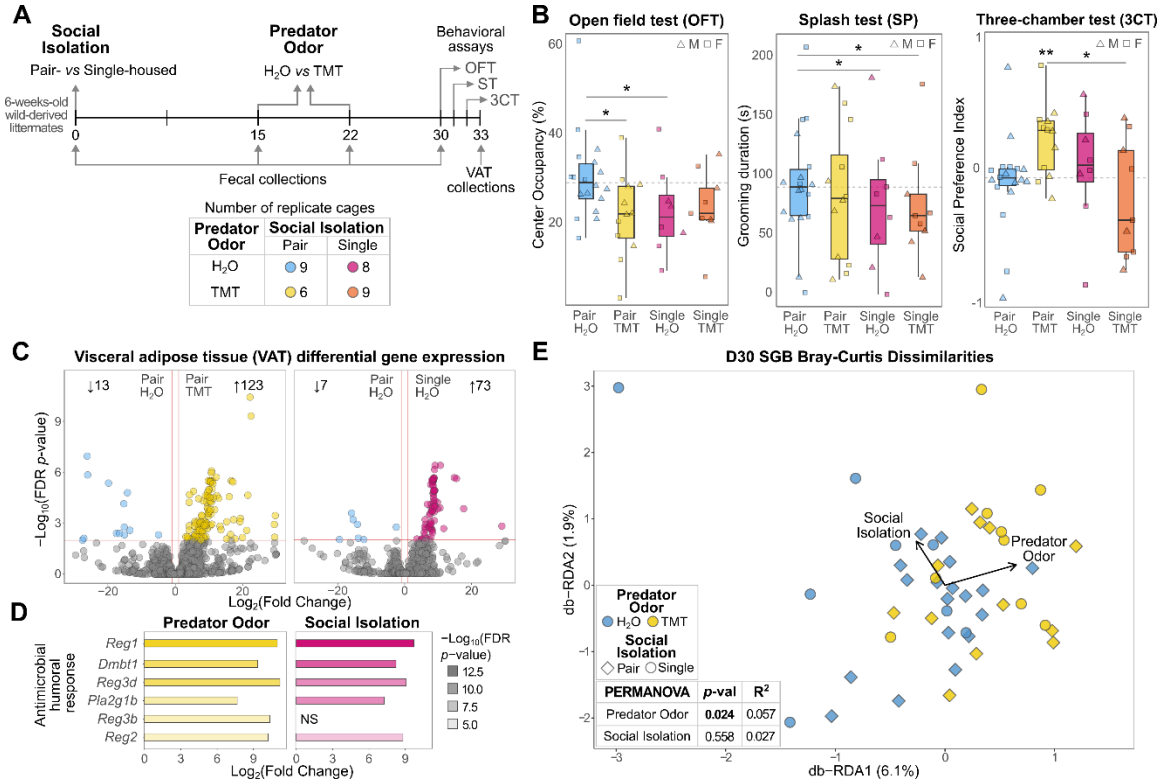

Figure 1. Predator-odor exposure altered host behavior, gene expression, and gut microbiota. (**A**) Diagram shows experiment timeline and number of cages per treatment group. (**B**) Box plots show, for male (triangles) and female (squares) mice, time spent in the central area of open-field tests (OFT), time spent grooming in splash tests (SP), and social preference index in three-chamber tests (3CT). Differences between stressor groups and unstressed controls were tested using linear mixed-effects models (LMM) accounting for sex, litter, and cage effects (* = $p < 0.05$). Differences between stressor groups were assessed by pairwise comparisons of LMM marginal means (* = FDR-adjusted $p < 0.05$). In the 3CT plot, we tested whether the social preference index within each group significantly differed from zero with a one-sample Wilcoxon test (** = $p < 0.01$). Dashed gray lines indicate unstressed controls' mean. (**C**) Volcano plots show log2-transformed fold change (LFC) in gene-expression level (points) in the visceral adipose tissue (VAT) of male and female mice in response to predator-odor exposure (left) or social isolation (right). Genes in the upper-outer quadrants were differentially expressed (DEGs; absolute

831 LFC > 1 and FDR-adjusted $p < 0.01$). The total number of DEGs is presented at the top of
832 each plot. (**D**) Bar plots show absolute LFC of genes belonging to the anti-microbial
833 humoral response biological pathway, which was found to be significantly enriched in the
834 up-regulated DEGs of mice exposed to predator odor (left) and social isolation (right).
835 Genes are ordered and colored by the $-\log_{10}$(FDR-adjusted p) resulting from differential
836 expression analyses. (**E**) Distance-based redundancy analysis (db-RDA) shows the first
837 two axes of constrained ordination of the Bray-Curtis dissimilarity matrix of species
838 genome bins (SGBs) composition at D30, accounting for sex and litter effects. Points
839 represent the SGB profiles of pair (diamond) and single-housed (circle) mice, colored by
840 whether they were exposed to H_2O (blue) or TMT (yellow). Vectors indicate direction and
841 relative strength of association between stressors and gut microbiome composition. The
842 percent variation explained by each axis is enclosed in parentheses.

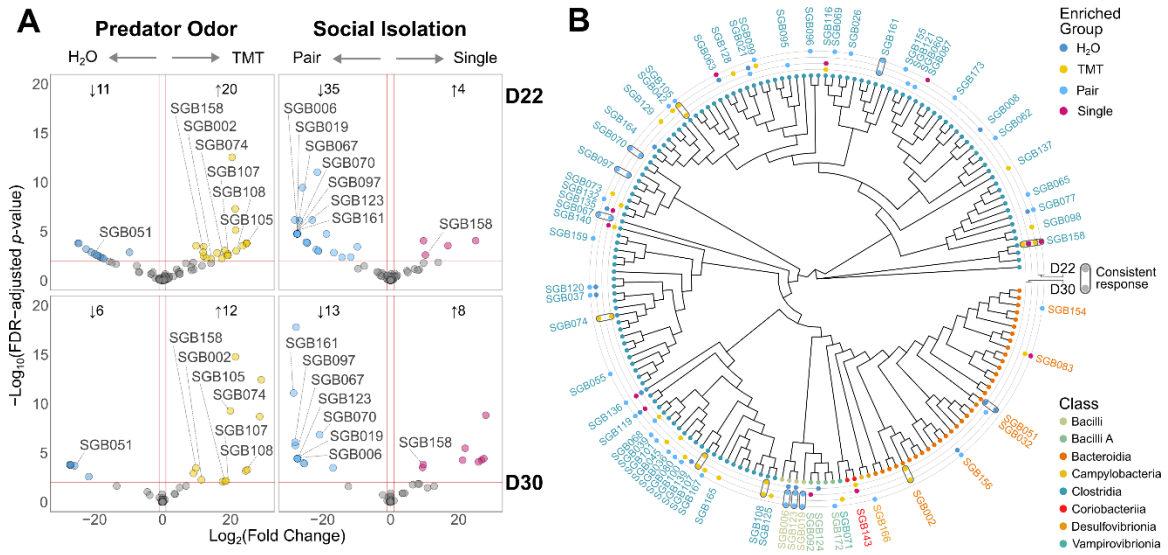

Figure 2. Predator-odor exposure drove consistent alterations in the relative abundances of specific SGBs. (**A**) Volcano plots show $\log_2$-transformed fold change (LFC) in the relative abundances of species genome bins (SGBs; points) in the gut microbiota in response to predator-odor exposure (left column) or social isolation (right column) a week after the first TMT exposure (D22; top row) and a week after the second TMT exposure (D30; bottom row). Upper-outer quadrants contain points corresponding to differentially abundant SGBs (DESeq2; absolute LFC > 1 and FDR-adjusted $p < 0.01$). The total number of differentially abundant SGBs is presented at the top of each plot. SGBs that responded consistently to the stressors at both D22 and D30 are labelled. (**B**) Phylogenetic tree shows evolutionary relationship (number of amino acid substitutions) between SGBs, with the tips colored by bacterial class. The rings show differentially abundant SGBs at D22 (outer two rings) and D30 (inner two rings), colored by the stressor group in which they were enriched: H_2O (dark blue) *vs.* TMT (yellow) and Pair (light blue) *vs.* Single (pink). SGBs that displayed a consistent response to the stressors across both D22 and D30 are encircled.

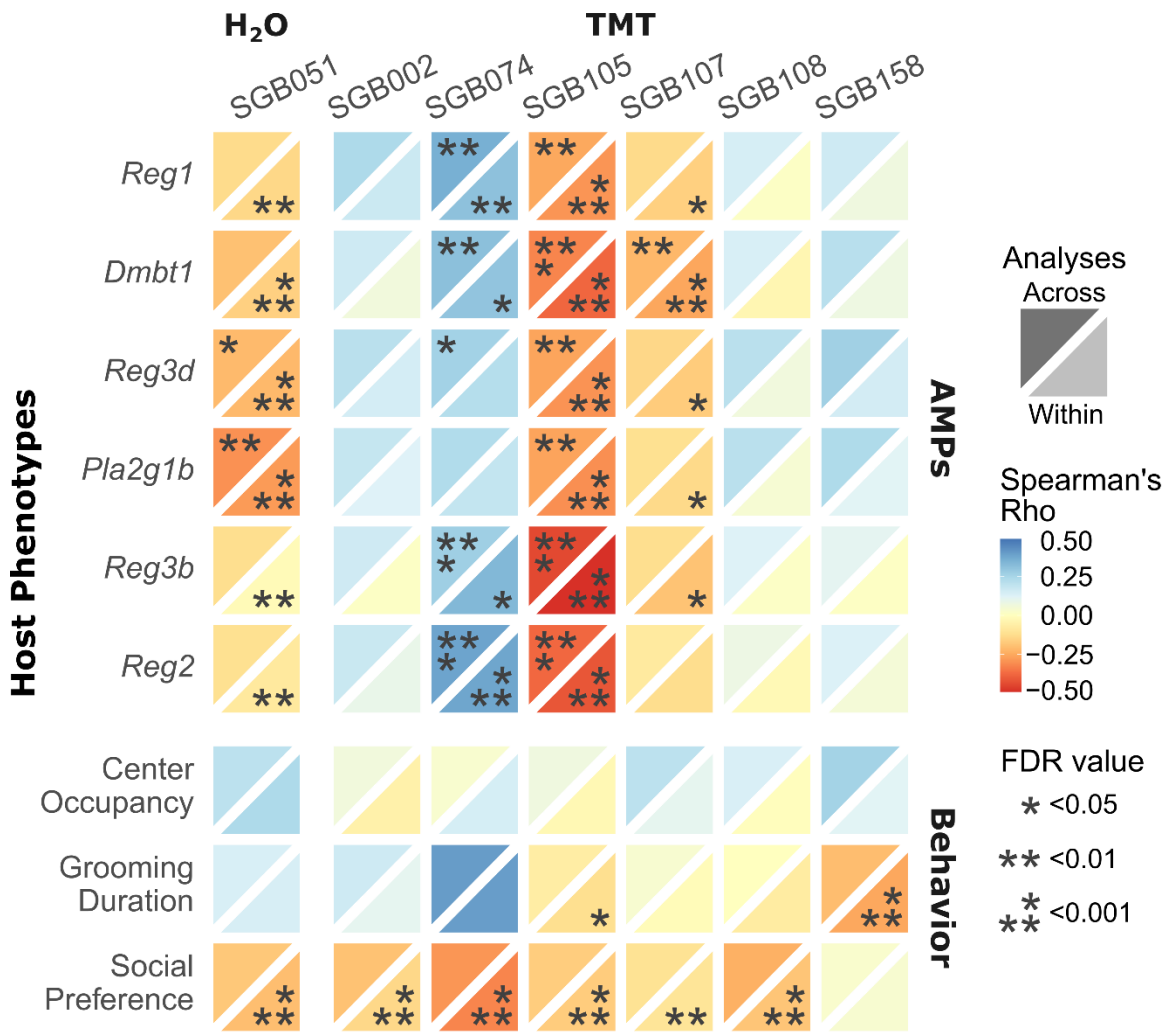

Figure 3. Predator odor–responsive SGBs co-varied with host anti-microbial and behavioral responses. Heatmap shows associations between the D22 relative abundances of SGBs that were consistently associated with predator-odor exposure (differentially abundant at both D22 and D30) and host anti-microbial (AMPs) and behavioral responses. The top facet represents correlations across treatment groups, and the bottom facet correlations within groups. Facets are colored according to Spearman's Rho and annotated with the correlation's FDR-adjusted *p*-value (* < 0.05; ** < 0.01; *** < 0.001).

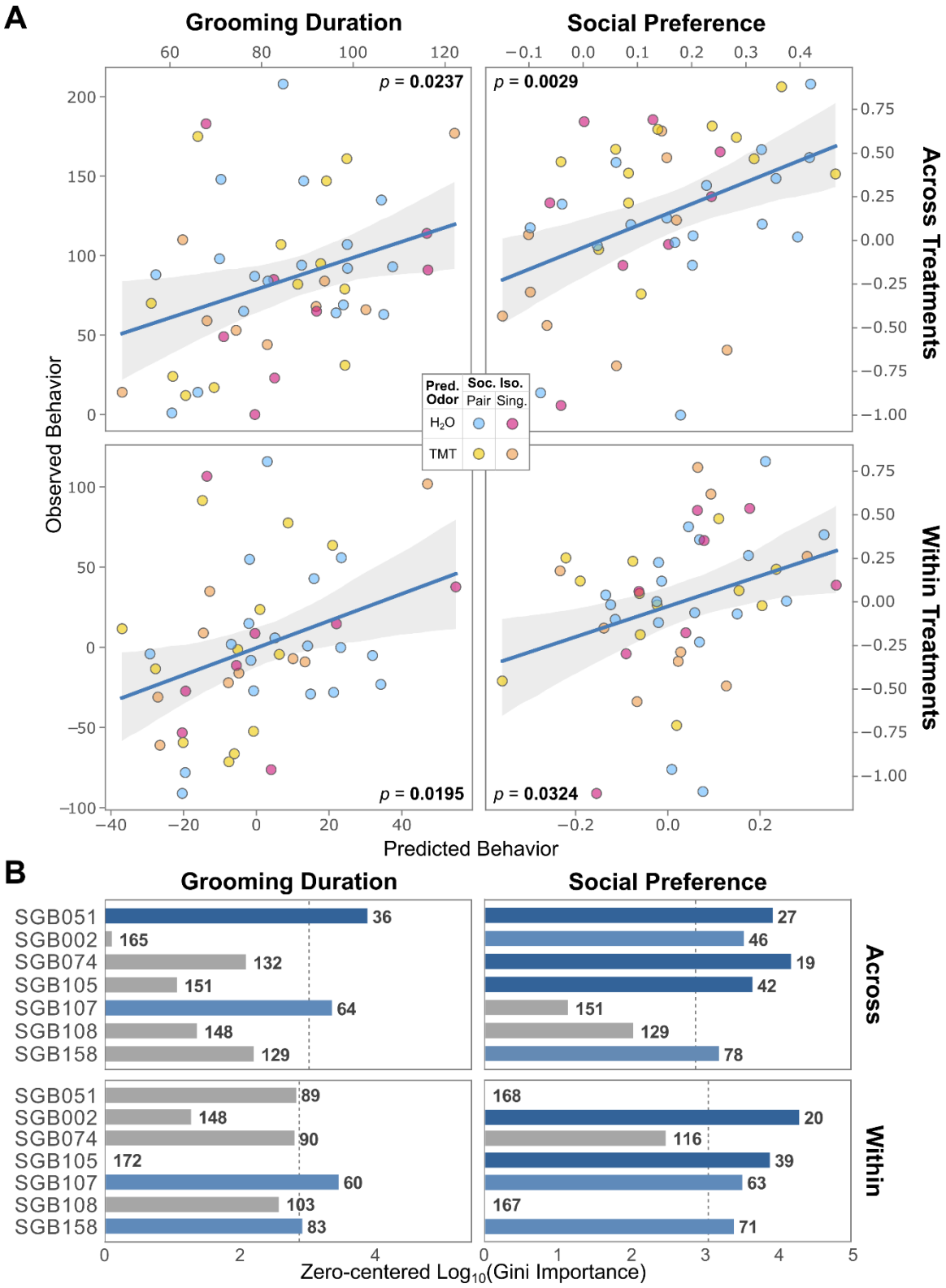
A
Grooming Duration
Social Preference
p = 0.0237
p = 0.0029
p = 0.0195
p = 0.0324
Across Treatments
Within Treatments
Observed Behavior
Predicted Behavior
Pred. Odor
Soc. Iso.
Pair
Sing.
H2O
TMT
B
Grooming Duration
Social Preference
SGB051
SGB002
SGB074
SGB105
SGB107
SGB108
SGB158
Across
Within
Zero-centered Log10(Gini Importance)

867

868 **Figure 4. Gut microbiota predicted host behavior.** (**A**) Scatter plots show the
869 relationships between observed grooming (left column) and social (right column) behavior
870 and the values predicted by a random forest model trained on SGB relative abundances at
871 D30, either across (top row) or within treatment groups (bottom row; behavior residualized
872 to account for the effect of stressor treatment). Points are colored by treatment group: blue,
873 Pair H_2O; yellow, Pair TMT; pink, Single H_2O; orange, Single TMT. The significance of
874 the linear regression is shown in the upper inner corner, with significant values ($p < 0.05$)
875 in bold. (**B**) Bar plots show the zero-centered $\log_{10}$(Gini Importance) of SGBs consistently
876 associated with predator-odor exposure (differentially abundant at both D22 and D30) for
877 predicting grooming (left) and social (right) behaviors both across (top) and within
878 (bottom) treatment groups. The SGB importance rank order is annotated in bold. The bars
879 are colored light blue if the SGB was among the top half most important features and dark
880 blue if among the top quarter. The dashed line indicates the median importance value.